

7.1 INTRODUCTION

In quite recent years, there has been an intense search for the materials which can up-convert the near infrared light to visible light. Such materials are very important because of their versatile applications in diversified fields such as fiber amplifiers, optoelectronic devices, lasers, color displays, optical data storage and under water optical communication [251]. In recent year's wavelength division multiplexing (WDM) technology gained so much of attention as it increases the information carrying capacity of communication network used in telecommunication systems [252-254]. Since broadband fiber amplifiers are the key devices in such systems, tremendous work has been dedicated in fabricating the optical materials possessing broad bandwidths of luminescence particularly in the wavelength range from 1200-2600 nm [255, 256]. For such near infrared and mid infrared applications, the materials in general are activated by RE ions. Quite recently, rare earth (RE) ions doped glasses are found to be potential in the development of luminescent devices suitable for Infrared (IR) lasers, infra-red to visible up-convertors, fiber and waveguide amplifiers for optical transmission network [252-254].

The glasses doped with rare earth ions became superior than crystals because of several advantages such as easy preparation, large RE³⁺ ion doping capacity, large inhomogeneous line broadening etc. [257]. The host materials used for rare-earth ions doping play a significant role for getting highly efficient up-conversions. It is well known that a host material with low phonon energies can suppress the non-radiative decay loss produced by multi-phonon relaxation and increases the luminescence efficiency. Strong up-conversion luminescence is possible in such systems having phonon energies considerably less. In the present investigation, using B₂O₃, Bi₂O₃, ZnO and Al₂O₃ chemicals as constituent elements we prepared ZnAlBiB glass in which Er³⁺ ions were placed with different concentrations to study the luminescence efficiency of these glasses in different regions of the electromagnetic spectrum. Excellent luminescent properties observed in these ZnAlBiB glasses doped with Dy³⁺, Sm³⁺, Ho³⁺, Tb³⁺ and Eu³⁺ ions motivated me to take up the present investigation [194, 195, 196, 258, 259].

Among all the RE ions, Er³⁺ ions are considered to be the most important ions because of their potential applications in the fields of optical fiber amplifiers, infrared lasers, microchip lasers, erbium doped fiber amplifiers (EDFA) in wavelength

division multiplexing (WDM) system, eye-safe lasers in medical fields [260]. This EDFA is one of the key devices for use in 1.5 μm wavelength optical communication window. The broadening of optical communication window system becomes very important because of the rapid increase of information carrying capacity and the need of flexible networks [261]. Recently, up-conversion emission studies of Er³⁺ ions in different mediums have been increased because of its visible green and red emissions. In Er³⁺ ions doped materials, the red up-conversion emission increases due to energy transfer (ET) between neighboring RE ions, whereas the green up-conversion emission is due to excited state absorption (ESA) as well as ET [74, 75]. On the other hand, at higher concentration of rare earth ions, the local surroundings of rare earth ions and optical properties of host glass matrix are influenced by clustering of rare earth ions. Such aggregation and clustering of rare earth ions will augment the interaction between rare earth ions resulting in luminescence quenching [76, 77]. The present work reports the results of the systematic investigation on the luminescence properties of ZnAlBiB glasses doped with different concentrations of Er³⁺ ions in different regions of the electromagnetic spectrum using absorption, emission, up-conversion and decay spectral measurements.

7.2 EXPERIMENTAL

Glasses with molar composition of 20 ZnO + 10 Al₂O₃ + (10-x) Bi₂O₃ + 60 B₂O₃ + x Er₂O₃ (where x=0.1, 0.5, 1.0 and 2.0 mol %) were prepared by melt quenching method. For convenience these glasses are labelled as ZnAlBiBEr01, ZnAlBiBEr05, ZnAlBiBEr10 and ZnAlBiBEr20 depending on the RE ion concentration present in the glass. By using the measured densities and refractive indices, several other physical properties were evaluated using the expressions collected from literature [226] and are given in Table 7.1. The absorption spectra of these glasses were recorded by using JASCO V-670 UV-vis-NIR spectrophotometer in the range of 300-1800 nm. The luminescence spectra of these glasses have been recorded using Shimadzu RF-5301 PC type spectrofluorophotometer. Fluorescence in NIR region was detected through an ANDOR SR-500i-B2 monochromator coupled to InGaAs detector through the suitable filters and lenses assembly. The up-conversion and fluorescence decay measurements were recorded using a monochromator (Acton

SP2300) coupled to CCD (charge coupled detector) through the appropriate lenses and filters by employing 980 nmlaser as an excitation source.

7.3 RESULT AND DISCUSSION

7.3.1. Optical Absorption spectral analysis

Figure 7.1 shows the optical absorption spectrum of ZnAlBiBER20 glass in the range 300-1800 nm. It has various inhomogeneous broadened bands due to f-f transitions which originate from 4f⁹ configuration of Er³⁺ ions. The absorption occurs due to 4f–4f electric dipole transitions from the ⁴I_{15/2} ground state to various excited state of Er³⁺ ions. The absorption spectrum shown in Figure 7.1, consists eleven absorption bands at wavelengths 1530, 977, 798, 658, 547, 522, 486, 449, 405, 376 and 372 nm corresponding to the transitions ⁴I_{15/2}→⁴I_{13/2}, ⁴I_{11/2}, ⁴I_{9/2} ⁴F_{9/2}, ⁴S_{3/2}, ²H_{11/2}, ⁴F_{7/2}, ⁴F_{5/2}, ²G_{9/2}, ⁴G_{11/2} and ²G_{7/2} respectively [262]. With Er³⁺ ion concentration in ZnAlBiB glasses, no change is observed in peak positions except some intensity variations.

The intensities of the absorption bands known as oscillator strengths (f_{exp}) are measured from the relative areas under the absorption bands using Eq. (1.5). The JO theory [79, 88] has been used to estimate the oscillator strengths (f_{cal}) of the absorption transitions from the ground level (Ψ_J) to various excited state ($\Psi'J'$) of Er³⁺ ions by using Eq. (1.9). The JO intensity parameters ($\Omega_{\lambda=2, 4, 6}$) were estimated by using the least square fitting approximation method, which can provide the essential information about the symmetry and bonding of the active ions within ligand fields [79, 88]. The experimental and calculated oscillator strengths (f_{exp} , f_{cal}) along with root mean square (δ_{rms}) deviation for Er³⁺ ion in ZnAlBiB glasses are given in Table 7.2.

Table 7.1: Physical properties of Er³⁺ ions in ZnAlBiB Glasses.

Physical properties	ZnAlBiBEr01	ZnAlBiBEr05	ZnAlBiBEr10	ZnAlBiBEr20
Refractive index (n_d)	1.821	1.819	1.816	1.811
Density (d) (g/cc)	3.906	3.905	3.904	3.901
Average molecular weight (\bar{M})(g)	114.7	114.4	114.4	114.0
Er ³⁺ ion concentration ($\times 10^{22}$ ions/cm ³)	0.205	1.027	2.054	4.122
Mean atomic Volume (g/cm ³ /atom)	6.676	6.658	6.660	6.640
Dielectric Constant (ϵ)	3.316	3.308	3.297	3.279
Optical Dielectric constant ($\epsilon - 1$)	2.316	2.308	2.297	2.279
Reflection losses (R %)	0.084	0.084	0.083	0.083
Molar Refraction (R_m)(cm ⁻³)	12.79	12.74	12.71	12.61
Polaron radius (r_p) (Å)	3.224	1.885	1.496	1.187
Interionic distance (r_i) (Å)	8.001	4.677	3.714	2.945
Molar electronic polarizability α ($\times 10^{-3}$ cm ³)	5.075	1.010	0.504	0.250
Field Strength ($\times 10^{15}$ cm ⁻²)	2.884	8.441	13.39	21.28
Optical basicity (Λ_{th})	0.438	0.439	0.441	0.445

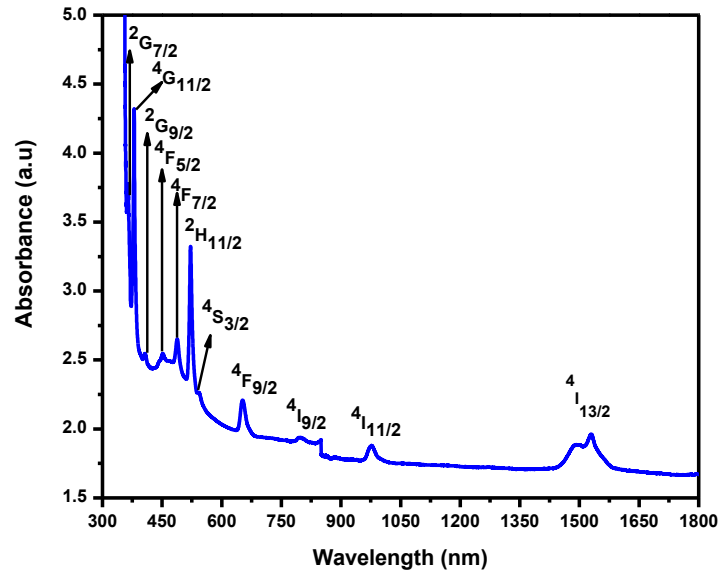


Figure 7.1 UV-vis-NIR absorption spectrum of ZnAlBiBER20 glass.

Table 7.2 Experimental (f_{exp}) ($\times 10^{-06}$) and calculated oscillator strength (f_{cal}) ($\times 10^{-06}$) of Er^{3+} ions in ZnAlBiB glasses.

Transition	Wave Energy (cm^{-1})	ZnAlBiBER01		ZnAlBiBER05		ZnAlBiBER10		ZnAlBiBER20	
		f_{exp}	f_{cal}	f_{exp}	f_{cal}	f_{exp}	f_{cal}	f_{exp}	f_{cal}
${}^4\text{I}_{15/2} \rightarrow$									
${}^4\text{I}_{13/2}$	6535	-	-	1.800	1.734	2.310	2.196	2.170	2.047
${}^4\text{I}_{11/2}$	10121	-	-	0.836	0.741	0.962	0.987	0.911	0.934
${}^4\text{I}_{9/2}$	12515	0.210	0.193	0.31	0.409	0.491	0.755	0.369	0.674
${}^4\text{F}_{9/2}$	15337	1.240	1.242	2.772	2.658	3.220	4.172	3.200	3.780
${}^4\text{S}_{3/2}$	18484	0.251	0.315	0.295	0.684	0.386	0.810	0.364	0.757
${}^2\text{H}_{11/2}$	19193	2.44	2.445	5.62	5.074	10.00	12.29	9.180	11.91
${}^4\text{F}_{7/2}$	20491	1.18	1.245	2.22	2.691	2.880	3.560	2.620	3.283
${}^4\text{F}_{5/2}$	21929	0.578	0.377	0.80	0.820	1.910	0.970	1.580	0.906
${}^2\text{G}_{9/2}$	24630	0.530	0.468	0.783	1.014	1.360	1.258	0.694	1.169
${}^4\text{G}_{11/2}$	26315	4.31	4.304	8.34	8.933	24.10	21.66	23.90	21.00
${}^2\text{G}_{7/2}$	27624	-	-	-	-	7.540	2.926	5.860	2.638
δ_{rms}		± 0.081		± 0.334		± 1.784		± 1.595	

The JO intensity parameters ($\Omega_{\lambda=2, 4, 6}$) obtained through least square fitting analysis are listed in Table 7.3. From Table 7.3, it is observed that the JO intensity parameters for all the ZnAlBiB glasses follow the same trend $\Omega_2 > \Omega_4 > \Omega_6$ in all glasses. In general the JO parameters are very sensitive to the structural change in the host matrix.

Table 7.3 Comparison of JO Parameters ($\Omega_2, \Omega_4, \Omega_6$) ($\times 10^{-20} \text{ cm}^2$), and their trend for Er^{3+} ions in ZnAlBiB glasses with other reported glass systems.

Glass System	Ω_2	Ω_4	Ω_6	Trend	References
ZnAlBiBEr01	1.02	0.72	0.66	$\Omega_2 > \Omega_4 > \Omega_6$	Present system
ZnAlBiBEr05	2.10	1.53	1.43	$\Omega_2 > \Omega_4 > \Omega_6$	Present system
ZnAlBiBEr10	5.82	2.90	1.70	$\Omega_2 > \Omega_4 > \Omega_6$	Present system
ZnAlBiBEr20	5.80	2.59	1.60	$\Omega_2 > \Omega_4 > \Omega_6$	Present system
YB25	3.86	1.52	1.17	$\Omega_2 > \Omega_4 > \Omega_6$	[266]
LiBO	3.24	0.92	0.82	$\Omega_2 > \Omega_4 > \Omega_6$	[267]
Germa-silicate	3.4	2.11	1.56	$\Omega_2 > \Omega_4 > \Omega_6$	[268]
Fluorophosphate	5.14	1.02	0.91	$\Omega_2 > \Omega_4 > \Omega_6$	[269]
Fluoride	3.08	1.46	1.69	$\Omega_2 > \Omega_4 > \Omega_6$	[270]
SNZE0.5	4.46	1.21	0.71	$\Omega_2 > \Omega_4 > \Omega_6$	[271]
$\text{SiO}_2 + \text{Na}_2\text{O}$	4.23	1.04	0.61	$\Omega_2 > \Omega_4 > \Omega_6$	[272]
SAL	5.59	1.42	0.87	$\Omega_2 > \Omega_4 > \Omega_6$	[273]
KTFP	5.09	0.69	1.47	$\Omega_2 > \Omega_6 > \Omega_4$	[260]
NKZLSEr10	5.82	2.35	2.37	$\Omega_2 > \Omega_6 > \Omega_4$	[274]

In the present case, the Ω_2 value is increasing with increase in Er^{3+} concentration up to 1 mol % and decreases beyond as shown in Figure 7.2. Usually Ω_2 is related to the degree of the covalency of the RE-O bond and as well as the asymmetry around the RE ion which in turn depends on the short range effects.

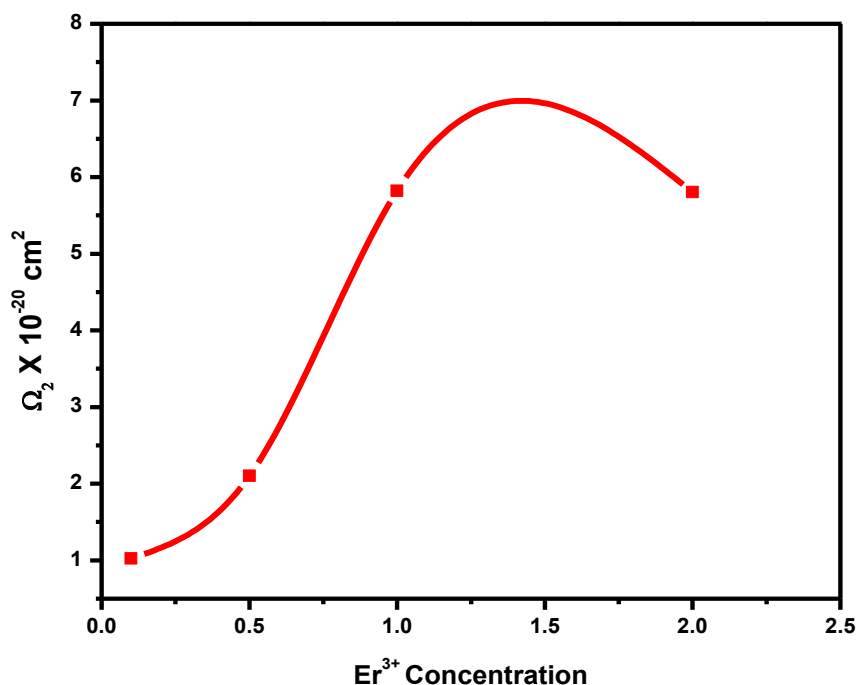


Figure 7.2. Variation of Ω_2 with respect to the Er^{3+} ion concentration in ZnAlBiB Glasses

From Table 7.3, it is observed that the Ω_2 value is high for ZnAlBiBER10 glass because of the superior oscillator strength of hypersensitive transitions. Hence ZnAlBiBER10 glass has the strong covalency of RE-O bond and highest asymmetry of the sites in the surrounding area of the dopant ion. Among the JO parameters, Ω_6 has least influence and Ω_4 has moderate influence on the structure of the host matrix due to the small values of $\|U^2\|^2$, $\|U^4\|^2$ square reduce matrix elements. Ω_4 and Ω_6 JO parameter values depend on the bulk properties of the medium such as viscosity and dielectric constant of the media and are also affected by the vibronic transitions of the RE ions bounded to the ligand atoms [263-265]. As given in Table 7.3, the JO parameter values obtained for the present glass systems are comparable with the values reported for other Er doped glassy systems [260, 266-274]. The JO parameters

obtained in the present work suggest that different concentrations of Er³⁺ ion in ZnAlBiB glasses possess strong asymmetry and/or covalency of the RE sites.

7.3.2. Absorption Edge

The study of optical absorption spectra gives very useful information about optically induced electronic transitions, energy gap and band structure of various crystalline and amorphous materials [275]. It is well known that, a material exposed for photons will absorb the energy continuously if the energy supplied is greater than the band gap energy of that material [260, 276]. Such energy absorption made by the glasses in UV-vis-NIR regions can be used to study the short-range structure of glasses which in turn gives the information of immediate surroundings of the absorbing atom [277]. Optical absorption edge is one of the important parameters used to describe solid state disordered materials and can be interpreted in terms of indirect transitions across optical band gap. According to Mott and Devis [272] the absorption coefficient is given by

$$\alpha(\nu) = \frac{B(h\nu - E_{opt})^n}{h\nu} \quad (7.1)$$

Where n is the index number used to specify the type of transition causing the absorption and E_{opt} is the optical band gap energy. Fig. 7.3 represents the tauc's plot indicating the variation of $(\alpha h\nu)^{1/2}$ with photon energy (hν) obtained by substituting the value n=1/2 in equation 2 corresponding to a transition. By extrapolating the linear region of the curves shown in Figure 7.3 at $(\alpha h\nu)^{1/2} = 0$, the band gap energy values for all the glasses under investigation were obtained. From Figure 7.3 it is observed that, the fundamental absorption edge slightly shifts toward the blue region with decreasing in Bi₂O₃ content which is may be due to some structural rearrangement in the glass brought by network former and modifier [278]. The optical band gap energy values for Er³⁺ ions doped ZnAlBiB glasses are found to be increasing with increase in Er³⁺ ion concentration (ZnAlBiBEr01- 2.32eV, ZnAlBiBEr05- 2.44eV, ZnAlBiBEr10- 2.92eV and ZnAlBiBEr20- 3.44 eV). Such results obtained for the present glasses suggests that the covalent nature of the glass matrix increases with increase in Er³⁺ ion concentration in the present titled glasses.

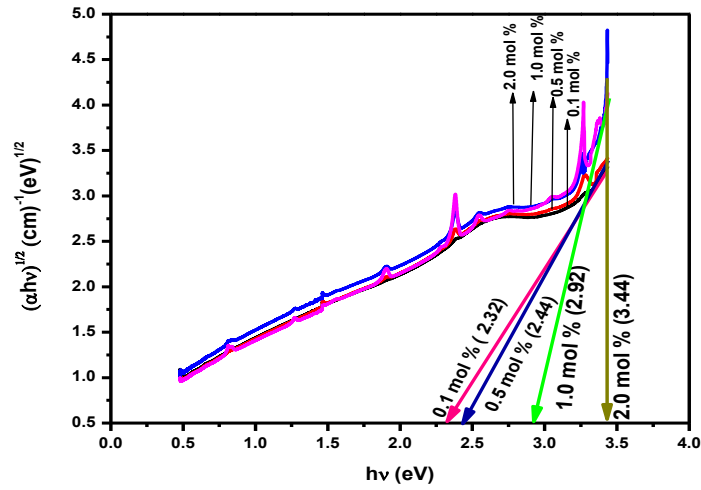


Figure 7.3. Variation of $(ah\nu)^{1/2}$ with photon energy ($h\nu$) in Er^{3+} ions in ZnAlBiB glasses

7.3.3 Visible, NIR Luminescence & Decay curve analysis:

In order to record the PL spectra, it is essential to identify the excitation bands for the prepared Er^{3+} ions doped ZnAlBiB glasses. Figure 7.4 shows the excitation spectra which consists of the three major excitation peaks at 347, 380, 478 nm corresponding to the transitions $^4\text{I}_{15/2} \rightarrow ^2\text{G}_{7/2}$, $^4\text{I}_{15/2} \rightarrow ^4\text{G}_{11/2}$ and $^4\text{I}_{15/2} \rightarrow ^4\text{F}_{7/2}$ respectively. Among the three excitation peaks shown in Figure 7.4, it is observed that $^4\text{I}_{15/2} \rightarrow ^4\text{G}_{11/2}$ transition at 380 nm is more intense and is used to record the PL spectra for all the ZnAlBiB glasses under investigation.

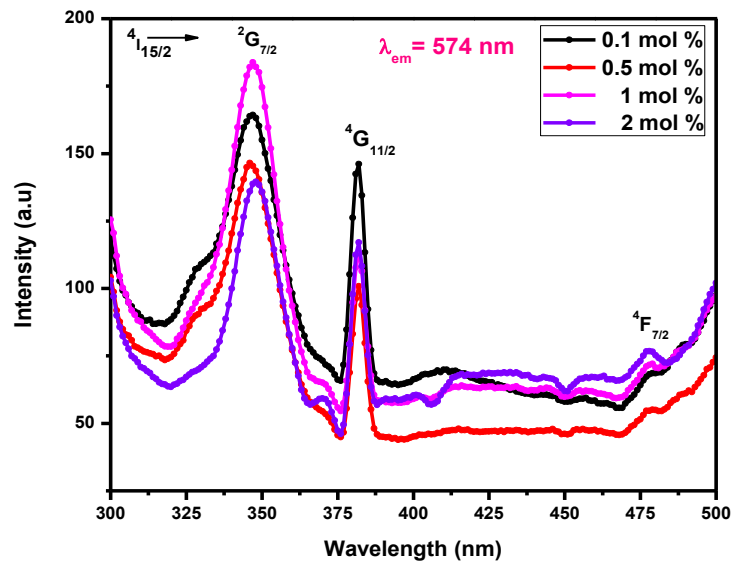


Figure 7.4 PL Excitation Spectra of Er^{3+} ions in ZnAlBiB glasses

Such luminescence spectra obtained for Er^{3+} ion in the ZnAlBiB glasses under 380 nm excitation wavelengths is shown in Figure 7.5. The non-radiative relaxation from ${}^4\text{G}_{11/2}$ level populates the ${}^4\text{S}_{3/2}$ and ${}^4\text{I}_{9/2}$ emitting states and the emissions occur from these levels to the ${}^4\text{I}_{15/2}$ ground level. The resultant spectra consist of two emission bands at 575 nm and 723 nm corresponding to ${}^4\text{S}_{3/2} \rightarrow {}^4\text{I}_{15/2}$ and ${}^4\text{I}_{9/2} \rightarrow {}^4\text{I}_{15/2}$ transitions respectively. From Figure 7.5 it can also be seen that, the intensity of the emission bands increases with increase in Er^{3+} ion concentration from 0.1 to 1.0 mol % and then decreases beyond showing quenching at 1 mol% of Er^{3+} ion concentration. The quenching in luminescence intensity may be due to a non-radiative energy transfer [279] mechanism.

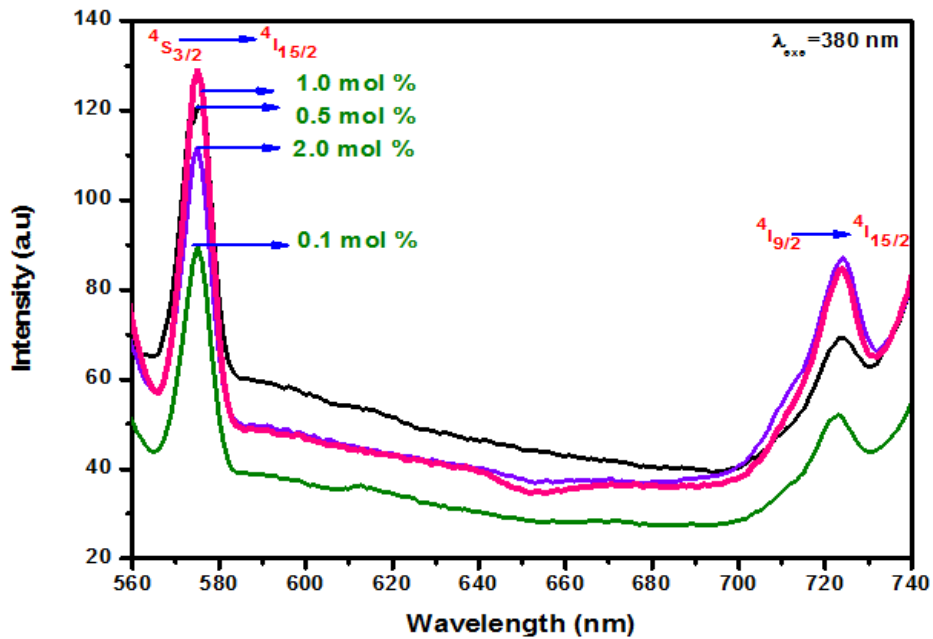


Figure 7.5 PL Emission Spectra of Er^{3+} ions in ZnAlBiB glasses

Among the two emission transitions, a transition observed in Green region (${}^4\text{S}_{3/2} \rightarrow {}^4\text{I}_{15/2}$) is highly intense than other transition observed in red region (${}^4\text{I}_{9/2} \rightarrow {}^4\text{I}_{15/2}$). From this luminescence spectra and JO parameters obtained from the absorption spectra, the important radiative properties such as radiative transition probabilities (A_R), radiative branching ratios (β_R), stimulated emission cross-sections (σ_{se}), radiative lifetime (τ_R), gain band width ($\sigma_{se} \times \Delta\lambda_p$) and optical gain parameters ($\sigma_{se} \times \tau_R$) are determined by using the relevant expressions given in Chapter 2 and are given in Table 7.4. From the data presented in Table 7.4, it can be seen that the stimulated emission cross-sections and branching ratios values are high for ${}^4\text{S}_{3/2} \rightarrow$

$^4I_{15/2}$ transition in ZnAlBiBER10 glass. This suggests that ZnAlBiBER10 glass is quite suitable to act as a good luminescent device in visible green region (575 nm) of the electromagnetic spectrum.

Table 7.4:

Emission peak wavelength (λ_p) (nm), effective band widths (FWHM) ($\Delta\lambda_p$) (nm), transition Probability (A_R) (s^{-1}), branching ratios (β_R & β_{exp}), stimulated emission cross-section (σ_{se}) ($\times 10^{20}$) (cm^2), radiative lifetime (τ_R) (ms), gain band width ($\sigma_{se} \times \Delta\lambda_p$) ($\times 10^{27}$) (cm^3) and optical gain ($\sigma_{se} \times \tau_R$) ($\times 10^{22}$) ($cm^2 s$) parameters evaluated from the visible emission spectra of Er^{3+} ions in ZnAlBiB Glasses.

Glass	$\Delta\lambda_p$	A_R	β_R	β_{exp}	σ_{se}	τ_R	$\sigma_{se} \times \Delta\lambda_p$	$\sigma_{se} \times \tau_R$
$^4S_{3/2} \rightarrow ^4I_{15/2}$ ($\lambda_p = 575$ nm)								
ZnAlBiBER01	6.15	971	0.6641	0.480	0.68	0.68	4.23	47.3
ZnAlBiBER05	4.61	2103	0.6646	0.483	2.00	0.31	9.22	63.4
ZnAlBiBER10	4.61	2480	0.667	0.563	2.37	0.26	10.9	63.1
ZnAlBiBER20	4.61	2306	0.667	0.527	2.22	0.28	10.2	63.9
$^4I_{9/2} \rightarrow ^4I_{15/2}$ ($\lambda_p = 723$ nm)								
ZnAlBiBER01	9.23	1051	0.589	0.437	0.17	0.85	1.59	117
ZnAlBiBER05	9.23	2245	0.588	0.472	0.25	0.40	2.35	81.9
ZnAlBiBER10	10.8	3522	0.567	0.561	0.40	0.25	4.35	79.2
ZnAlBiBER20	9.23	3172	0.575	0.519	0.42	0.28	3.90	92.2

The near infrared (NIR) luminescence spectra of Er^{3+} doped ZnAlBiB glasses have been recorded by using 980 nm laser as an excitation source and are shown in Figure 7.6. The NIR luminescence spectra show a strong emission peak at 1530 nm corresponding to the transition ${}^4I_{13/2} \rightarrow {}^4I_{15/2}$. The intensity of this emission transition increases with increase in Er^{3+} ion concentration up to 1 mol% and then decreases.

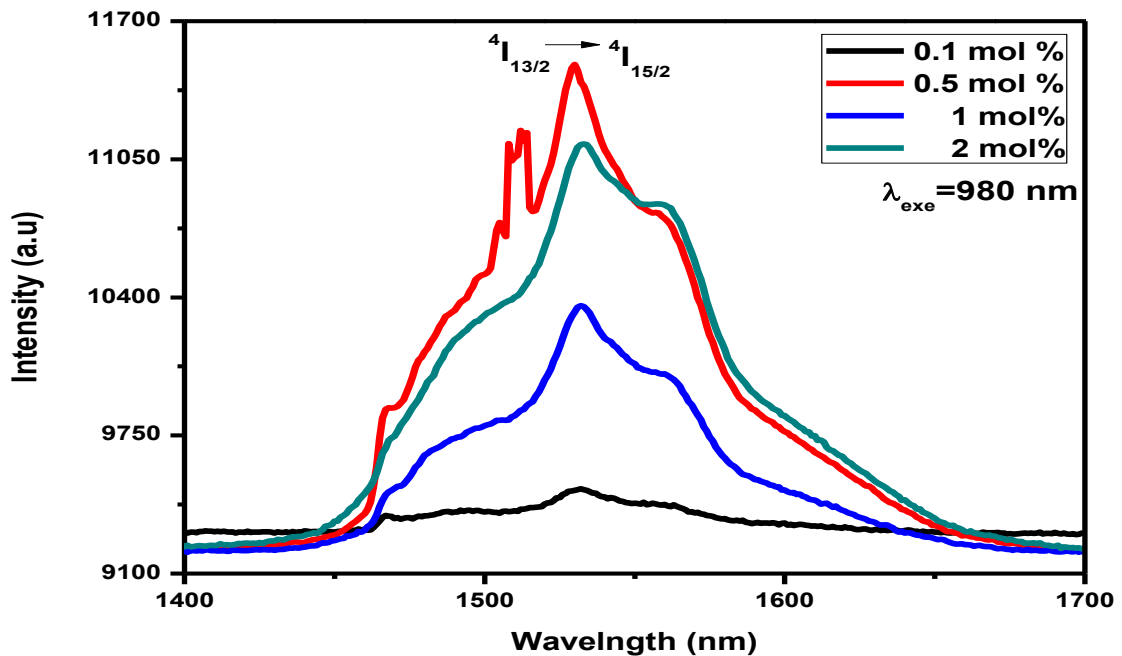


Figure 7.6 NIR fluorescence spectra of Er^{3+} ions in ZnAlBiB glasses

To have a comprehensive picture on the emission characteristics of the Er^{3+} ions in ZnAlBiB glasses, we have evaluated the important radiative parameters such as full width at half maxima (FWHM) ($\Delta\lambda_p$), stimulated emission cross-section (σ_{se}), gain band width ($\Delta\lambda_p \times \sigma_{se}$) and optical gain parameters ($\tau_R \times \sigma_{se}$) [28] and are given in Table 7.5. Large values of FWHM are very much useful in optical fiber amplifiers to enhance the number of possible optical channels that can be multiplexed without the usage of any gain compensation technique in WDM systems [281]. The product of full width at half maxima and stimulated emission cross-section ($\text{FWHM} \times \sigma_{se}$) is often used to calculate the bandwidth of optical fiber amplifier [282]. From Table 7.5 it is observed that among all the titled glasses, the ZnAlBiBEr10 glass possesses maximum values for all these parameters. The stimulated emission cross-section and gain band width values of ZnAlBiBEr10 glass are comparable to the other reported glass hosts [274, 283-287].

Table 7.5:

Comparison of emission peak wavelength (λ_p) (nm), effective band widths ($\Delta\lambda_p$) (nm), stimulated emission cross-section (σ_{se}) ($\times 10^{21}$) (cm^2), radiative and experimental lifetimes (τ_R, τ_{exp}) (ms), Quantum efficiency (η) (%), gain band width ($\sigma_{se} \times \Delta\lambda_p$) ($\times 10^{28}$) (cm^3) and optical gain ($\sigma_{se} \times \tau_R$) ($\times 10^{25}$) ($\text{cm}^2 \text{ s}$) parameters for the NIR emission of Er^{3+} ions in ZnAlBiB glasses.

Glass System	λ_p	$\Delta\lambda_p$	σ_{se}	τ_R	τ_{exp}	η	$\sigma_{se} \times \Delta\lambda_p$	$\sigma_{se} \times \tau_R$
ZnAlBiBEr01	1530	81.9	3.89	0.68	0.41	59	31.9	2.67
ZnAlBiBEr05	1530	67.5	7.99	0.40	0.37	74	54.0	3.25
ZnAlBiBEr10	1530	57.0	11.4	0.34	0.31	91	64.9	3.87
ZnAlBiBEr20	1530	65.5	9.38	0.36	0.30	82	61.5	3.39
NKZLSEr10 [274]	1540	93.0	0.74	-	-	-	6.94	-
LiTFP [283]	1534	37.9	1.12	-	-	-	42.7	-
NaTFP [283]	1534	39.3	1.17	-	-	-	45.9	-
KTFP [283]	1534	36.4	1.24	-	-	-	45.2	-
Silicate [284]	-	40.0	0.55	-	-	-	2.20	-
GaBPGe [285]	-	58.0	1.03	-	-	-	5.97	-
Tellurite [286]	-	59.0	0.68	-	-	-	4.06	-
GaBP1[287]	-	62.0	1.03	-	-	-	6.38	-
Phosphate[286]	-	56.0	0.67	-	-	-	3.79	-

In order to understand the 1.50 μm emission property, the absorption and emission cross-sections were also measured. These cross-sections tell us about the ability of the doped RE ions to absorb or emit light. It is well known that large stimulated emission cross-section gives high gain coefficient with low threshold energy needed for effective pumping action in lasers. Thus, in order to have a host aptly suitable for lasing action and optical fiber amplification, it is necessary to enhance the emission cross-section as high as possible [288]. The absorption and emission cross-sections of ZnAlBiBER10 glass has been calculated from the absorption spectrum and McCumber theory [289]. Figure 7.7 shows the absorption and emission cross sections of ZnAlBiBER10 glass. The absorption cross-sections of $^4I_{15/2} \rightarrow ^4I_{13/2}$ transition have been evaluated from the absorption spectrum using the following expression

$$\sigma_a(\lambda) = \frac{2.303 \text{ OD}(\lambda)}{Nl} \quad (7.2)$$

Where OD (λ), N, l represents the optical density (obtained from the absorption spectrum), Er^{3+} doping concentration and sample thickness, respectively.

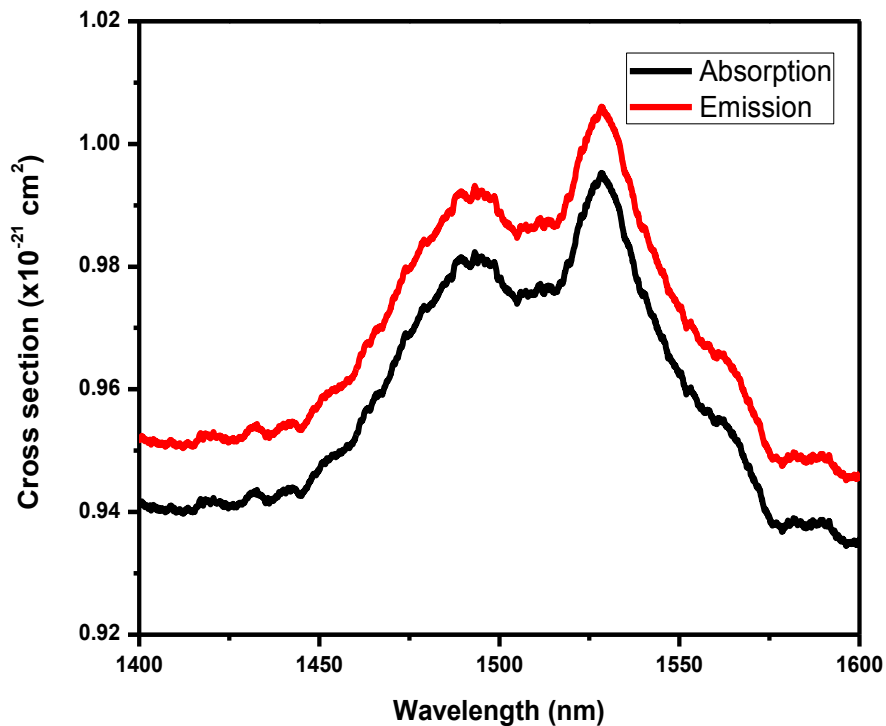


Figure 7. 7: Absorption and emission cross sections of ZnAlBiBER10 glass.

The stimulated emission-cross section of ${}^4I_{13/2} \rightarrow {}^4I_{13/2}$ transition is calculated using the equation given by McCumber theory [289].

$$\sigma_e(\lambda) = \sigma_a(\lambda) \exp\left(\frac{\varepsilon - h\nu}{kT}\right) \quad (7.3)$$

Where ε is the net free energy required to excite Er^{3+} from ${}^4I_{15/2}$ to ${}^4I_{13/2}$ state at temperature T . It can be calculated by the simplified procedure provided in Ref [290]. $\sigma_a(\lambda)$ and $\sigma_e(\lambda)$ are absorption and emission cross-sections respectively, h is the Planck constant, K the Boltzmann constant and ν is the phonon frequency. The calculated peak emission cross-section for ZnAlBiBER10 glass is $10.417 \times 10^{-22} \text{ cm}^2$ from the McCumber theory is in good agreement with the emission cross-section calculated from JO theory ($11.4 \times 10^{-22} \text{ cm}^2$). Hence this glass can be used for optical fiber amplification. The transient PL behavior of ${}^4I_{13/2} \rightarrow {}^4I_{15/2}$ emission transition measured for Er^{3+} ions in ZnAlBiB glasses is shown in Fig 8. From Fig 8, It is interesting to see that the photoluminescence decay of ${}^4I_{13/2}$ level is found to be single exponential in nature for all the glasses studied irrespective of the Er^{3+} ion concentration. The effective decay time (τ_{eff}), which is also called as experimental lifetime (τ_{exp}) has been evaluated from the recorded decay profiles using the following expression [291]

$$\tau_{\text{eff}} = \tau_{\text{exp}} = \frac{\int tI(t)dt}{\int I(t)dt} \quad (7.4)$$

The obtained experimental lifetime (τ_{exp}) values are given in Table 7.5. In general, the lifetime of ${}^4I_{13/2}$ level of Er^{3+} ion is strongly influenced by both radiative and non-radiative emission processes. In the present investigation the experimental lifetime (τ_{exp}) values measured from decay curves are found to be smaller than the radiative lifetimes (τ_{rad}) obtained from JO analysis.

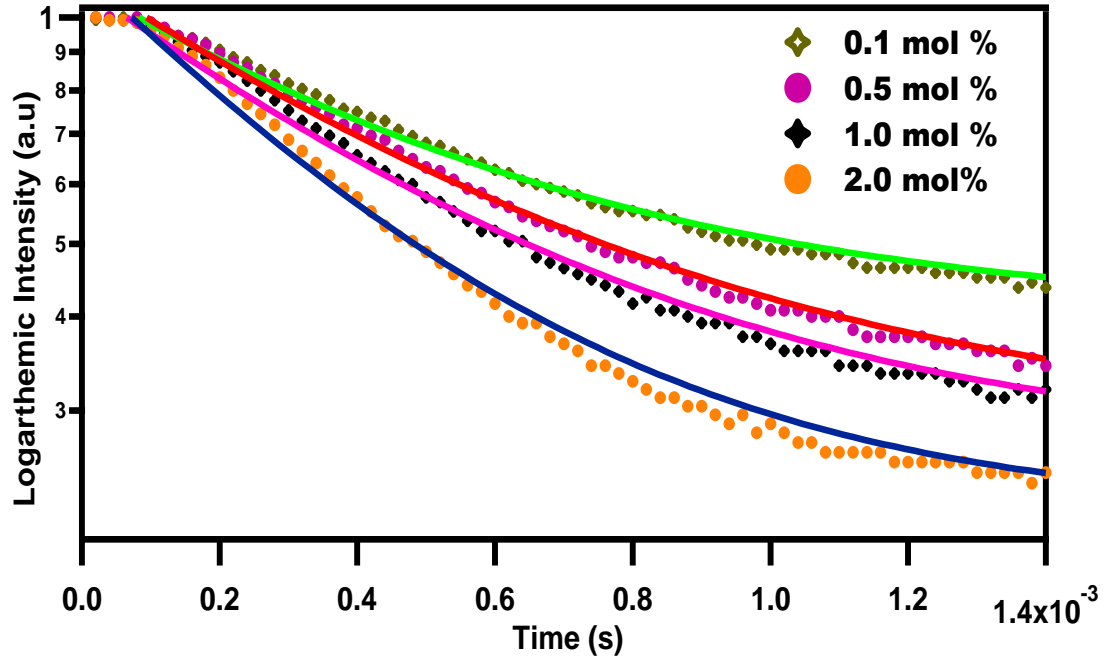


Figure 7.8 Decay curves of ${}^4I_{13/2} \rightarrow {}^4I_{15/2}$ emission transition of Er^{3+} ions in ZnAlBiB glasses ($\lambda_{\text{em}}=1530$ nm and $\lambda_{\text{exe}}=980$ nm)

The smaller values obtained for experimental lifetimes for the present glasses indicate that the relaxation mechanism from ${}^4I_{13/2}$ level is a combination of both radiative and non-radiative emission processes. The decrease in measured lifetimes with increase in Er^{3+} ion concentration in the present study may be attributed to the energy transfer among the neighbouring Er^{3+} ions and also energy transfer from Er^{3+} ions to quenching centers like OH^- groups [292, 293]. The Quantum efficiency (η) of the ${}^4I_{13/2}$ level can be estimated by using the Eq (1.27), and are given in Table 7.5.

From Table 7.5 it can be observed that, among all the Er^{3+} ions doped ZnAlBiB glasses, ZnAlBiBER10 glass possess highest values of stimulated emission cross-section, gain parameters and quantum efficiency values for the transition ${}^4I_{13/2} \rightarrow {}^4I_{15/2}$ (1530 nm). Hence ZnAlBiBER10 glass can be suggested as a good host to generate efficient lasing action at 1530 nm and also highly useful for optical fiber amplification.

7.3.4 Up-Conversion Luminescence Spectral analysis

Figure 7.9 shows the up-conversion luminescence spectra of Er^{3+} ions doped ZnAlBiB glasses under 980 nm laser excitation. The up-conversion luminescence spectra consist of two intense luminescence bands at 543 nm (green region) and 656 nm (red region) corresponding to the transitions $^4\text{S}_{3/2} \rightarrow ^4\text{I}_{15/2}$ and $^4\text{F}_{9/2} \rightarrow ^4\text{I}_{15/2}$ respectively. Among the two emission bands, a band observed in red region is more intense than green region. The intensity of this red band ($^4\text{F}_{9/2} \rightarrow ^4\text{I}_{15/2}$) increases with increase in the concentration of Er^{3+} ions up to 1 mol% and then decreases beyond showing the concentration quenching.

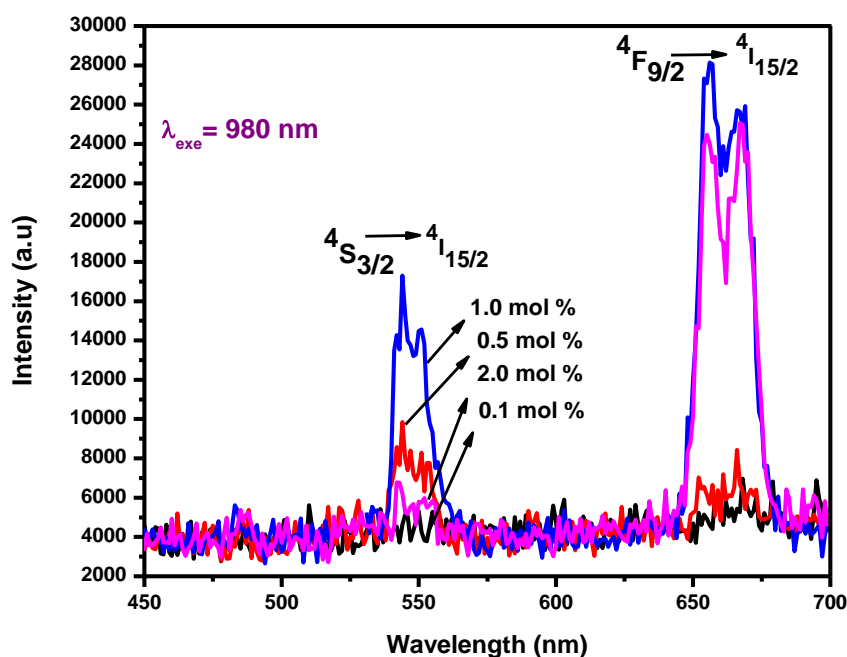


Figure 7.9 Up-conversion Emission spectra of Er^{3+} ions in ZnAlBiB glasses.

The possible up-conversion mechanism for the observed emission bands can be clearly understood from the energy levels diagram of ZnAlBiBER10 glass shown in Figure 7.10.

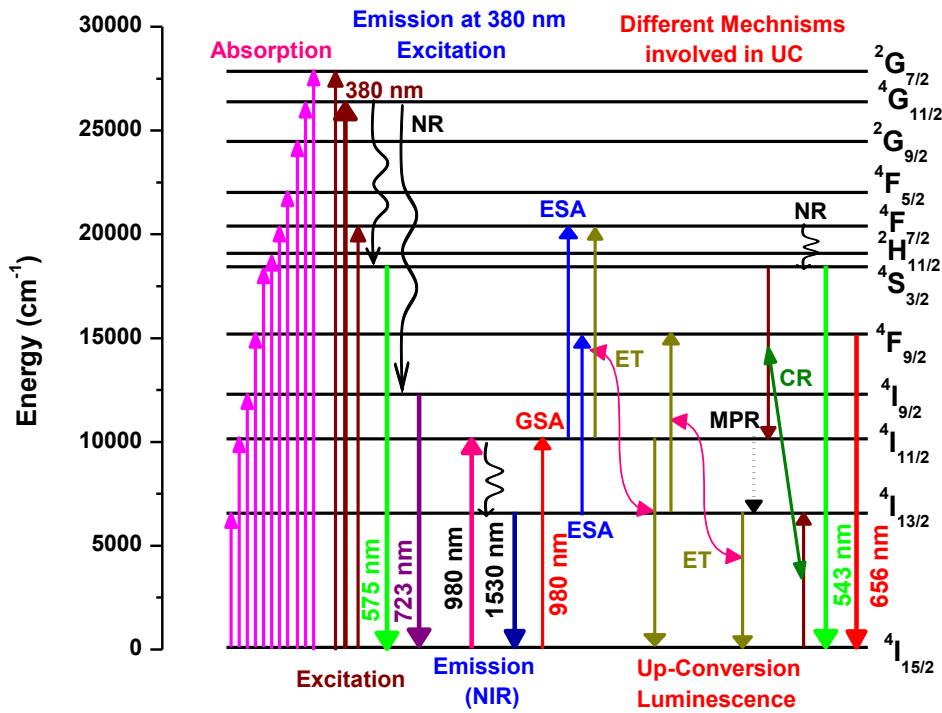


Figure 7.10 Energy level diagram of ZnAlBiB:Er³⁺ glass showing the mechanism of up conversion emission under 980nm excitation.

The mechanism of up-conversion observed in the present Er³⁺ ions doped ZnAlBiB glasses can be explained as follows. Generally, in up-conversion phenomenon, two photon process populates the atoms from ground state to the desired higher energy levels. Initially, under 980 nm laser excitation the Er³⁺ ions reaches to the ⁴I_{11/2} excited state from ⁴I_{15/2} ground state through the ground state absorption (GSA) mechanism [294].

Ground state absorption (GSA): ${}^4I_{15/2}(\text{Er}^{3+} \text{ ion}) + h\nu \text{ (a photon)} \rightarrow {}^4I_{11/2}(\text{Er}^{3+} \text{ ion})$

From ⁴I_{11/2} level the same ions by absorbing a second photon will move to ⁴F_{7/2} level by excited state absorption (ESA) and Energy transfer (ET) which can be represented by the simple processes as follows [294]

Excited State Absorption (ESA): ${}^4I_{11/2}(\text{Er}^{3+} \text{ ion}) + h\nu \text{ (a photon)} \rightarrow {}^4F_{7/2}(\text{Er}^{3+} \text{ ion})$

Energy Transfer (ET): ${}^4I_{11/2}(\text{Er}^{3+} \text{ ion}) + {}^4I_{11/2}(\text{Er}^{3+} \text{ ion}) \rightarrow {}^4F_{7/2}(\text{Er}^{3+} \text{ ion}) + {}^4I_{15/2}(\text{Er}^{3+} \text{ ion})$

Simultaneously Er^{3+} ion at the ${}^4\text{F}_{7/2}$ level decays very rapidly to the ${}^4\text{S}_{3/2}$ level through non-radiatively (NR) and subsequently the ${}^4\text{S}_{3/2} \rightarrow {}^4\text{I}_{15/2}$ transition emits an intense green up-conversion at 543 nm [294]. For the 656 nm red emission, Er^{3+} ions are excited to ${}^4\text{I}_{11/2}$ state through the GSA and energy transfer (ET) between adjacent Er^{3+} ions under 980 nm excitation. The populated Er^{3+} ions from ${}^4\text{I}_{11/2}$ state then decays to the long-living ${}^4\text{I}_{13/2}$ state via multi-phonon relaxation (MPR) and ultimately excited to the ${}^4\text{F}_{9/2}$ state by one of the following processes [294].

Multi-Phonon Relaxation: ${}^4\text{I}_{13/2} (\text{Er}^{3+} \text{ ion}) + h\nu (\text{a photon}) \rightarrow {}^4\text{I}_{11/2} (\text{Er}^{3+} \text{ ion})$

Energy Transfer: ${}^4\text{I}_{13/2} (\text{Er}^{3+} \text{ ion}) + {}^4\text{I}_{13/2} (\text{Er}^{3+} \text{ ion}) \rightarrow {}^4\text{I}_{15/2} (\text{Er}^{3+} \text{ ion}) + {}^4\text{F}_{9/2} (\text{Er}^{3+} \text{ ion})$

Finally, the ${}^4\text{F}_{9/2} \rightarrow {}^4\text{I}_{15/2}$ transition gives bright red color emission at 656 nm.

Table 7.6 gives the information pertaining to several important radiative properties such as peak wavelength, FWHM, stimulated emission cross-section, gain band widths and optical gain parameters evaluated from the up-conversion luminescence spectra. From Table 6 it is observed that among all the Er^{3+} ions doped ZnAlBiB glasses investigated in the present work, the ZnAlBiBEr10 glass possess highest stimulated emission cross-section, gain band width and optical gain parameters for the transition ${}^4\text{F}_{9/2} \rightarrow {}^4\text{I}_{15/2}$ (656 nm) in bright red region. Hence ZnAlBiBEr10 glass can be suggested as a good host for giving up-conversion luminescence in the red region corresponding to the transition ${}^4\text{F}_{9/2} \rightarrow {}^4\text{I}_{15/2}$ at 656 nm under 980 nm laser excitation.

Table 7.6:

Emission peak wavelength (λ_p) (nm), effective band widths ($\Delta\lambda_p$) (nm), stimulated emission cross-section (σ_{se}) ($\times 10^{-21}$) (cm^2), gain band width ($\sigma_{se} \times \Delta\lambda_p$) ($\times 10^{28}$) (cm^3) and optical gain ($\sigma_{se} \times \tau_R$) ($\times 10^{20}$) ($\text{cm}^2 \text{s}$) parameters for the up-conversion emission transitions of Er^{3+} ions in ZnAlBiB Glasses.

Glass	λ_p	$\Delta\lambda_p$	σ_{se}	$\sigma_{se} \times \Delta\lambda_p$	$\sigma_{se} \times \tau_R$
$^4\text{S}_{3/2} \rightarrow ^4\text{I}_{15/2}$ (Green)					
ZnAlBiBEr01	543	26.92	1.25	33.7	0.859
ZnAlBiBEr05	543	23.07	3.18	73.3	1.01
ZnAlBiBEr10	543	13.46	6.44	86.8	0.172
ZnAlBiBEr20	543	21.15	3.85	81.4	0.111
$^4\text{F}_{9/2} \rightarrow ^4\text{I}_{15/2}$ (Red)					
ZnAlBiBEr01	656	28.8	2.69	77.6	2.30
ZnAlBiBEr05	656	25.0	6.67	167	2.68
ZnAlBiBEr10	656	21.2	12.4	262	0.319
ZnAlBiBEr20	656	23.1	10.3	238	0.295

7.4. CONCLUSION

In the present study, Zinc Alumino Bismuth Borate (ZnAlBiB) glasses doped with different concentrations of Er^{3+} ions were successfully prepared by using the conventional melt quenching technique to characterize their effective usage for visible and NIR applications using spectroscopic techniques such as absorption, excitation, luminescence, PL decay and up-conversion luminescence. The increase in optical band gap values also show a strong covalency of Er^{3+} ion in the glass network. The

visible luminescence under 380 nm excitation wavelength show two emission bands at 575 nm and 723 nm corresponding to the transitions $^4S_{3/2} \rightarrow ^4I_{15/2}$ and $^4I_{9/2} \rightarrow ^4I_{15/2}$ respectively. Among these two transitions, a transition at 575 nm is more intense than other one and possesses highest values of branching ratio, stimulated emission cross-section and optical gain parameters for the glass ZnAlBiBER10. Hence ZnAlBiBER10 glass can be suggested as good optical material to emit green luminescence. The NIR PL spectra recorded under 980 nm laser excitation source show one broad peak at 1530 nm corresponding to the transition $^4I_{13/2} \rightarrow ^4I_{15/2}$. Among all the ZnAlBiB glasses under investigation, ZnAlBiBER10 glass possesses maximum values of branching ratio, stimulated emission cross-section, gain bandwidth and optical gain parameters. The nearly broad and flat nature of 1530 nm NIR emission and the other favorable radiative optical properties possessed by ZnAlBiBER10 glass suggests the possibility of using this glass for broadband optical fiber amplification applications. The up-conversion luminescence spectra recorded under the excitation wavelength 980 nm show two emission bands in green and red regions corresponding to the transitions $^4S_{3/2} \rightarrow ^4I_{15/2}$ (543 nm) and $^4F_{9/2} \rightarrow ^4I_{15/2}$ (656 nm) respectively. Among these two transitions, a transition observed in red region found to be more intense than green and the luminescent parameters for this transition also found to be highest for ZnAlBiBER10 glass. Hence this glass can be suggested as suitable material for visible up-conversion laser applications. Our systematic spectroscopic analysis taken up for ZnAlBiB glasses doped with Er^{3+} ions at different concentrations allows us to contemplate that these glasses are potential candidates for luminescent applications in different regions of the electromagnetic spectrum. Especially, ZnAlBiB glass doped with 1mol% of Er^{3+} ions can act as an efficient luminescent device among all the glasses studied in visible and NIR regions. The same glass also acts as good up-conversion luminescent device under 980 nm laser excitation.